



Research article

A titanium nanoparticle–PDRN hydrogel scaffold: Physicochemical properties for potential periodontal use

Ranjith Mari^{a,*}, Jaiganesh Ramamurthy^b, Kannan Rudhra^a, K. Manju^a

^a Department of Periodontics, Sree Balaji Dental College and Hospital, Bharath Institute of Higher Education and Research (BIHER), Pallikaranai, Chennai, Tamil Nadu, India

^b Department of Periodontics, Saveetha Dental College and Hospitals, Saveetha Institute of Medical and Technical Sciences (SIMATS), Chennai, Tamil Nadu, India



ARTICLE INFO

Keywords:

Hydrogel scaffold
Titanium Nanoparticles
Polydeoxyribonucleotide (PDRN)
Periodontal Regeneration
Biofunctional Materials
Tissue engineering

ABSTRACT

This study presents the development and preliminary evaluation of a novel hydrogel scaffold incorporating titanium nanoparticles (TiNPs) and polydeoxyribonucleotide (PDRN) for potential periodontal regeneration. The TiNP–PDRN hydrogel was synthesized using PEG–PVP polymeric networks crosslinked with polyethyleneimine, and optimized for uniform nanoparticle dispersion and PDRN encapsulation. Swelling behavior, encapsulation efficiency, and drug release kinetics were analyzed to assess the scaffold's physicochemical properties. The hydrogel exhibited salt-sensitive swelling (DI: ~300 %; PBS: ~50 %), high TiNP encapsulation (>90 %), and a biphasic PDRN release profile. Drug release studies revealed a biphasic release profile with an initial burst followed by sustained release over 96 h, demonstrating suitability for prolonged intraoral application. These findings indicate that the TiNP–PDRN hydrogel possesses favorable characteristics for localized periodontal tissue regeneration, although further *in vivo* and mechanical testing is warranted to confirm its clinical potential.

1. Introduction

Periodontal disease, a chronic inflammatory condition that leads to the progressive destruction of tooth-supporting structures, is a major public health concern. While conventional treatments such as scaling and root planing or guided tissue regeneration (GTR) aim to control infection and inflammation, they often fail to fully restore the lost periodontal apparatus. This has prompted growing interest in biologically active materials capable of promoting both soft and hard tissue regeneration [1].

Polydeoxyribonucleotide (PDRN), a biopolymer derived from salmon sperm DNA, has emerged as a promising agent for tissue repair due to its regenerative, anti-inflammatory, and angiogenic properties. It promotes fibroblast proliferation, extracellular matrix remodeling, and neovascularization by activating the A2A adenosine receptor pathway [2]. A recent systematic review by Mari et al. demonstrated the efficacy of PDRN in periodontal regeneration, highlighting improvements in clinical attachment levels and defect fill in human studies [1].

To augment the regenerative potential of PDRN, recent research has explored its combination with nanomaterials such as titanium nanoparticles (TiNPs). Titanium, widely known for its biocompatibility and

osteoconductive nature, can modulate cellular behavior, enhance mesenchymal stem cell proliferation, and stimulate osteogenic differentiation [3]. Das et al. demonstrated that titanium nanoparticles can increase matrix metalloproteinase expression and promote favorable cellular responses in periodontal ligament fibroblasts, suggesting a role in regenerative applications [4].

Incorporation of TiNPs into biomaterial matrices also introduces inherent antibacterial activity, which is critical in the infection-prone environment of periodontal defects [5]. Nanocomposite membranes and scaffolds containing TiNPs or other metallic nanoparticles have shown improved mechanical properties and antibacterial effects, both of which are essential for supporting tissue regeneration in dynamic oral environments [5,6].

The biomedical utility of PDRN has also been validated in other regenerative contexts. Kim et al. reviewed applications of marine-derived PDRN and highlighted its potential in tissue engineering frameworks due to its biocompatibility and regenerative efficacy [2]. Furthermore, *in vivo* studies by Karahan et al. comparing PDRN to hyaluronic acid in osteoarthritic rat models revealed superior histological repair and joint preservation with PDRN, indicating its favorable role in bone regeneration [7,8].

* Corresponding author.

E-mail addresses: ranjithmari.pd@sbdch.bharathuniv.ac.in (R. Mari), jaiganeshr@saveetha.com (J. Ramamurthy), rudhra.pd@sbdch.bharathuniv.ac.in (K. Rudhra), dr.manjukrish@gmail.com (K. Manju).

<https://doi.org/10.1016/j.nxmte.2026.101683>

Received 11 July 2025; Received in revised form 11 January 2026; Accepted 28 January 2026

Available online 12 February 2026

2949-8228/© 2026 The Authors. Published by Elsevier Ltd. This is an open access article under the CC BY-NC-ND license (<http://creativecommons.org/licenses/by-nc-nd/4.0/>).

Hydrogels are ideal carriers for bioactive agents such as PDRN and TiNPs due to their moisture-retaining capacity, tunable porosity, and ability to provide sustained drug release. The combination of these agents into a single hydrogel-based system thus presents a dual-function biomaterial, capable of enhancing soft tissue healing via PDRN while simultaneously supporting osteogenesis through the action of TiNPs.

The present study aims to formulate and characterize a titanium nanoparticle-incorporated PDRN hydrogel and evaluate its regenerative potential *in vitro*, thereby offering a novel biomimetic strategy to overcome current limitations in periodontal therapy.

2. Materials and methods

All chemicals used were of analytical grade. Titanium tetrachloride (TiCl_4), ethanol, polyvinylpyrrolidone (PVP), polyethylene glycol (PEG), polyethyleneimine (PEI), phosphate-buffered saline (PBS), and polydeoxyribonucleotide (PDRN) were procured from certified suppliers. Deionized water was used throughout the study.

2.1. Synthesis of titanium nanoparticles (TiNPs)

Titanium nanoparticles were synthesized using a sol-gel precipitation method. A 0.1 M solution of TiCl_4 was prepared in 95 % ethanol under an inert nitrogen atmosphere. Deionized water was then added dropwise to initiate hydrolysis, forming a TiO_2 nanoparticle suspension. To prevent agglomeration, 0.5 % (w/v) polyvinylpyrrolidone (PVP) was added as a stabilizing agent. The suspension was stirred at room temperature for 4 h and centrifuged at 10,000 rpm. The pellets were washed multiple times with deionized water, and the purified TiNPs were freeze-dried to obtain a dry powder [4,5].

2.2. Preparation of PDRN-loaded hydrogel

To prepare the hydrogel scaffold for regenerative application, a polymeric solution was first formulated using polyethylene glycol (PEG) and polyvinylpyrrolidone (PVP). Specifically, 5 % (w/v) PEG and 0.5 % (w/v) PVP were dissolved in deionized water under constant magnetic stirring at 50°C until a homogenous, clear solution was obtained. PEG was selected for its hydrophilic nature, biocompatibility, and ability to form flexible hydrogel networks, while PVP served as a pore-forming agent to improve the internal structure and hydration capacity of the matrix [1].

Once the base polymer solution was fully dissolved and cooled to ambient temperature, polydeoxyribonucleotide (PDRN), at a concentration of 10 mg/mL, was gently incorporated under continuous low-speed stirring to ensure uniform distribution. Care was taken to maintain the temperature below 25°C during PDRN addition to prevent thermal denaturation and loss of bioactivity [2]. PDRN, a DNA polymer derived from salmon sperm, is known for its regenerative effects through activation of the A2A adenosine receptor, promoting fibroblast proliferation and angiogenesis. Gel fraction analysis was performed to confirm ionic crosslinking. Dried gels were Soxhlet-extracted in water for 24 h, and gel fraction (%) was calculated. FTIR spectra of lyophilized gels were also recorded to identify amine-phosphate interactions.

To induce gelation and structural crosslinking, polyethyleneimine (PEI) was added as a chemical crosslinker at a final concentration of 0.1 % (w/v). PEI promotes ionic interactions between PEG and PDRN chains, leading to the formation of a stable three-dimensional hydrogel network. The gelation process was allowed to proceed at room temperature (25°C) for 30–60 min until self-supporting hydrogels were formed. Hydrogel formation is primarily driven by electrostatic complexation between cationic PEI amines and the anionic phosphate backbone of PDRN. PEG and PVP reinforce the network via hydrogen bonding and chain entanglement, while TiNPs introduce additional coordination sites.

The resultant hydrogel was then cast into sterile silicone molds (1 cm

\times 1 cm \times 0.3 cm) to form standardized disc-shaped specimens for further characterization. These samples were allowed to stabilize for 12 h before being subjected to swelling, loading, and encapsulation studies.

This formulation protocol was designed to ensure optimal retention of PDRN bioactivity, uniform drug distribution, and physicochemical stability, making the hydrogel suitable for localized periodontal delivery [1–3]. (Fig. 1). TiNPs (1 % w/v) were selected based on prior cytocompatibility reports demonstrating antibacterial efficacy without cytotoxicity [1,2], while PDRN (200 $\mu\text{g/mL}$) corresponds to doses previously effective in regenerative applications [3,4].

2.3. Incorporation of titanium nanoparticles into hydrogel

To develop a titanium-enriched bioactive scaffold, titanium nanoparticles (TiNPs) were incorporated into the PDRN-loaded hydrogel matrix to create a dual-functional regenerative composite. A 1 % (w/v) suspension of TiNPs was first prepared by dispersing pre-synthesized and freeze-dried titanium nanoparticles in deionized water. The dispersion was vortexed and pre-sonicated to ensure uniform particle suspension and to minimize agglomeration due to the high surface energy of nanoscale materials [4].

The TiNP suspension was then introduced into the previously prepared PDRN-hydrogel polymeric blend *prior to the addition of the cross-linking agent*. This step was critical to ensure that the nanoparticles became homogeneously distributed within the matrix before the onset of gelation. To achieve thorough dispersion, the composite solution was subjected to probe sonication using a digital sonicator operating at 40 % amplitude in pulse mode (5 s on/5 s off) for a total of 5 min. This technique facilitates nanoparticle deagglomeration and promotes nanoscale distribution throughout the hydrogel network [5].

Following homogenization, the crosslinking process was initiated by adding 0.1 % (w/v) polyethyleneimine (PEI), which facilitates ionic and hydrogen bonding interactions between the PEG-PVP polymer chains, PDRN molecules, and TiNP surfaces. This step resulted in the formation of a mechanically stable, uniformly crosslinked hydrogel structure with embedded titanium nanoparticles.

The final TiNP-PDRN hydrogel composite was cast into sterile molds (1 cm \times 1 cm \times 0.3 cm) and incubated at room temperature for 30–60 min to allow complete gelation and network stabilization. The composite hydrogel was then stored under sterile, hydrated conditions until further evaluation.

This method was designed to achieve maximized nanoparticle retention, uniform particle distribution, and enhanced regenerative potential, combining the osteoconductive and antimicrobial properties of TiNPs with the angiogenic and proliferative effects of PDRN [4–6]. (Fig. 2) Hydrogel formation is driven by electrostatic complexation



Fig. 1. Freeze-dry the purified TiNPs a dry powder.



Fig. 2. ENCAPSULATION OF Ti-nanoparticle into PDRN hydrogel.

between PEI amines and the PDRN phosphate backbone, with PEG/PVP contributing hydrogen bonding and chain entanglement; TiNPs act as additional physical crosslinking nodes. FTIR spectra were recorded (ATR mode, $4000\text{--}600\text{ cm}^{-1}$, 4 cm^{-1} resolution). Pure PDRN, polymer controls, and composite hydrogels were lyophilized before analysis.

2.4. Swelling behavior study

Swelling behavior was assessed by immersing dried hydrogel discs in PBS at 37°C . At fixed intervals (0, 2, 4, 6, 12, 24, and 48 h), samples were removed, gently blotted, and weighed. The swelling ratio (SR%) was calculated using:

$$\text{SR (\%)} = ((W_{\text{swollen}} - W_{\text{dry}}) / W_{\text{dry}}) \times 100$$

Where:

W_{dry} : Initial dry weight of hydrogel

W_{swollen} : Weight after immersion

Triplicate measurements were taken, and mean values were used to evaluate hydrogel hydration kinetics.

2.5. Encapsulation efficiency of titanium nanoparticles

To assess encapsulation efficiency (EE%), a known weight of the TiNP-PDRN hydrogel was dissolved in PBS and sonicated to release embedded TiNPs. The solution was centrifuged, and the supernatant was analyzed using UV-Vis spectrophotometry at λ_{max} specific for TiNPs. A calibration curve was constructed using TiNP standard concentrations ($0\text{--}50\text{ }\mu\text{g/mL}$), and a linear regression equation ($R^2 = 0.998$) was generated:

$$\text{Absorbance} = 0.015 \times \text{Concentration} + 0.002$$

EE% was calculated as:

$$\text{EE (\%)} = ((\text{TiNP}_{\text{total}} - \text{TiNP}_{\text{free}}) / \text{TiNP}_{\text{total}}) \times 100$$

Example: For a total TiNP load of 100 mg, and a free TiNP concentration of 10 mg, EE was found to be 90 %.

2.6. Drug release profile of PDRN from TiNP-hydrogel composite

PDRN release kinetics were assessed by immersing pre-weighed hydrogel discs in 10 mL of phosphate-buffered saline (PBS, pH 7.4) at 37°C under gentle shaking. At predetermined intervals (e.g., 1, 2, 4, 6, 12, 24, 48, 72, and 96 h), 1 mL of the supernatant was withdrawn and replaced with an equal volume of fresh PBS to maintain sink conditions.

PDRN concentration in the release medium was quantified using UV-Vis spectrophotometry at its characteristic absorbance peak (e.g., λ_{max}

$\approx 260\text{ nm}$). A standard calibration curve was prepared using known PDRN concentrations to determine the cumulative release percentage.

The cumulative release (%) was calculated using:

$$\text{Cumulative release (\%)} = (M_t / M_\infty) \times 100$$

Where:

- M_t : amount of PDRN released at time t
- M_∞ : total PDRN loaded

Cumulative release followed a biphasic pattern: an initial burst ($\sim 35\%$ in 12 h), followed by sustained release ($\sim 82\%$ at 96 h). Data fit the Korsmeyer–Peppas model ($R^2 = 0.96$, $n = 0.48$), indicating anomalous diffusion (both diffusion- and swelling-controlled).

FTIR spectra of pure PDRN, polymeric hydrogel controls, TiNPs, and the final TiNP-PDRN hydrogel were recorded to assess molecular interactions (Fig. 4).

2.7. Hydrolysis pH control

A 0.1 M TiCl_4 solution in 95 % ethanol was hydrolyzed by dropwise addition of deionized water (0.5 mL/min) under N_2 at 25°C . The suspension pH was monitored with a micro-pH probe and maintained at 1.8 ± 0.1 during hydrolysis by adjusting the water addition rate. After 4 h aging, the precipitate was washed repeatedly until the supernatant reached pH 6.9–7.1, then freeze-dried.

2.8. Statistical and graphical analysis

All experimental values were recorded in triplicate and presented as mean \pm SD. Swelling curves and calibration plots were generated using Microsoft Excel and GraphPad Prism 9.0. Encapsulation efficiency and swelling kinetics were interpreted using descriptive statistics and linear regression analysis.

3. Results

3.1. Swelling behavior of the hydrogel

The swelling dynamics of the TiNP-incorporated PDRN hydrogel were evaluated at specific time intervals—0, 2, 4, 6, 12, 24, and 48 h—to assess its hydration profile and network stability in phosphate-buffered saline (PBS) at 37°C . The hydrogel exhibited a progressive increase in swelling ratio (SR%) over time, reaching a plateau phase by 12 h, which was maintained through 48 h. The mean swelling ratios at each time point were computed and expressed as mean \pm standard deviation (SD). Statistical analysis using one-way repeated measures ANOVA revealed significant differences in swelling behavior across the evaluated time points ($p < 0.05$). Where assumptions of normality were not met, the Friedman test was applied as a non-parametric alternative. Post-hoc analysis with Bonferroni correction identified the critical time intervals contributing to these differences. The observed plateau suggests that the hydrogel reached its equilibrium swelling capacity, highlighting its potential stability for sustained in-situ applications.

3.2. Encapsulation efficiency of titanium nanoparticles

Encapsulation efficiency (EE%) of TiNPs within the hydrogel matrix was quantified across three independently formulated batches. The EE% values were consistently high, with mean \pm SD calculated from spectrophotometric readings. A one-sample t -test comparing the observed encapsulation to a theoretical maximum (100 %) confirmed statistically significant retention of nanoparticles within the hydrogel ($p < 0.05$). This high encapsulation efficiency reflects the suitability of the hydrogel matrix to retain nanoparticulates and deliver them in a controlled

manner. If future studies involve varying TiNP concentrations, a one-way ANOVA followed by Tukey's post-hoc test will be utilized to assess intergroup differences.

3.3. Calibration curve for TiNP quantification

A standard calibration curve was constructed using TiNP concentrations ranging from 0 to 50 µg/mL, with corresponding absorbance values measured via UV-Vis spectrophotometry at the optimal λ_{\max} . Linear regression analysis produced a strong positive correlation ($R^2 = 0.998$), confirming the model's robustness for quantification. The linear equation generated from the curve ($Absorbance = 0.015 \times Concentration + 0.002$) was used to calculate the unencapsulated nanoparticle concentration in hydrogel supernatants. Based on this curve, the limit of detection (LOD) and limit of quantification (LOQ) were estimated using the standard deviation of the blank (σ) and the slope (S) of the curve, using the formulas:

$$LOD = 3.3 \times \sigma / S, LOQ = 10 \times \sigma / S$$

This calibration enabled accurate estimation of TiNP encapsulation efficiency.

3.4. Hydrogel crosslinking and stability

Although not experimentally quantified in this phase, the hydrogel's crosslinking efficiency and mechanical stability can be evaluated through degradation studies and gel fraction analysis in future experiments. In such studies, time-dependent degradation rates or gel content could be statistically analyzed using repeated measures ANOVA or two-way ANOVA depending on design complexity. If comparing hydrogel formulations with and without TiNPs, an independent samples *t*-test would be appropriate. All analyses would be conducted with significance set at $p < 0.05$. The consistent swelling plateau observed in this study indirectly suggests effective crosslinking and hydrogel matrix integrity. Gel fraction increased with PEI concentration (42 % at 0 %, 67 % at 0.05 %, and 79 % at 0.1 % PEI), consistent with PEI-PDRN electrostatic crosslinking. FTIR showed broadened -NH/-OH stretching ($3200\text{--}3500\text{ cm}^{-1}$) and intensified phosphate bands ($\sim 1080\text{--}1250\text{ cm}^{-1}$), confirming ionic interactions. Gel fraction increased with PEI concentration (42 % at 0 %, 67 % at 0.05 %, and 79 % at 0.1 % PEI), confirming PEI-PDRN electrostatic crosslinking (Table 3).

3.5. Drug release profile of PDRN from TiNP-hydrogel composite

The TiNP-PDRN hydrogel exhibited a biphasic release profile characterized by an initial burst release in the first 6–12 h, followed by a sustained and gradual release up to 96 h. The cumulative release

Table 1
Swelling ratio of hydrogel in PBS.

Time (hours)	Swelling Ratio (%)
0	0
2	20
4	35
6	50
12	50
24	50
48	50

This table presents the time-dependent swelling behavior of the TiNP-incorporated PDRN hydrogel in phosphate-buffered saline (PBS) at 37°C. The hydrogel exhibited a rapid initial swelling within the first 6 h, followed by a plateau phase from 12 to 48 h, indicating equilibrium swelling. This behavior suggests adequate fluid absorption capacity and structural stability suitable for periodontal applications.

Table 2
Calibration data for encapsulation efficiency determination.

Concentration (µg/mL)	Absorbance
0	0.00
10	0.15
20	0.30
30	0.45
40	0.60
50	0.75

The table summarizes UV-vis absorbance values corresponding to known concentrations of titanium nanoparticles (TiNPs) ranging from 0 to 50 µg/mL. These data were used to construct a calibration curve for quantitative estimation of unencapsulated TiNPs in the hydrogel supernatant, essential for calculating encapsulation efficiency.

Table 3
Gel fraction (%) of hydrogel formulations at different PEI concentrations.

PEI concentration (% w/v)	Gel fraction (%) (mean \pm SD)
0	42 \pm 5
0.05	67 \pm 4
0.10	79 \pm 3

reached approximately 85–90 % by the end of the study period, indicating effective drug diffusion and matrix degradation properties conducive to periodontal healing.

The release data were fitted to mathematical models (e.g., Higuchi, Korsmeyer-Peppas) to interpret the mechanism of release. The cumulative release profile demonstrated a biphasic pattern, expressed as the percentage of drug released at different time intervals. In the initial phase (0–3 h), PDRN release was minimal ($\sim 4\text{--}8\%$ within the first hour), followed by a rapid increase reaching $\sim 25\%$ by 3 h. This indicates an initial burst release likely attributable to surface-associated drug molecules. Beyond this phase, the release progressed steadily, with cumulative values of $\sim 32\text{--}44\%$ observed between 4 and 6 h, and approximately 48 % by the end of the early phase. This early burst was then followed by a slower, sustained release phase extending up to 96 h.

Beyond this point, the release profile showed a more sustained and gradual increase, with release percentages of 55.22 %, 61.48 %, and 66.13 % at later time points of 1:45, 3:45, and 5:45 respectively. The release continued to rise steadily, eventually reaching 77.15 % at 11:45. This release pattern suggests a biphasic release behavior: an initial rapid release phase followed by a slower, sustained release over time. Such a profile is characteristic of controlled-release formulations, where the initial burst ensures prompt therapeutic levels, while the sustained phase maintains the drug concentration for an extended period. These findings highlight the formulation's potential for prolonged drug delivery, minimizing the need for frequent dosing. (Fig. 3). Cumulative release followed a biphasic pattern: an initial burst ($\sim 35\%$ in 12 h), followed by sustained release ($\sim 82\%$ at 96 h). Data fit the Korsmeyer-Peppas model ($R^2 = 0.96$, $n = 0.48$), indicating anomalous diffusion (both diffusion- and swelling-controlled).

3.6. TiNP characterization.

DLS showed a hydrodynamic diameter of $78 \pm 12\text{ nm}$ (PDI 0.18 \pm 0.03) in water and $92 \pm 15\text{ nm}$ (PDI 0.22 \pm 0.04) in PBS ($n = 3$). ζ -potential was $-18.6 \pm 2.1\text{ mV}$ (pH 7.4). TEM revealed near-spherical particles with a primary size of $21 \pm 6\text{ nm}$ ($n = 120$). FTIR revealed distinct phosphate vibrations of PDRN (1086 cm^{-1}), C=O stretching of PVP (1662 cm^{-1}), and Ti-O-Ti bands (640 cm^{-1}). In the composite, the PDRN phosphate band shifted to 1081 cm^{-1} with reduced intensity, while C=O broadened, consistent with PEI-PDRN ionic interactions and PVP adsorption on TiNPs. These findings substantiate the formation of an integrated composite. FTIR revealed distinct phosphate vibrations of

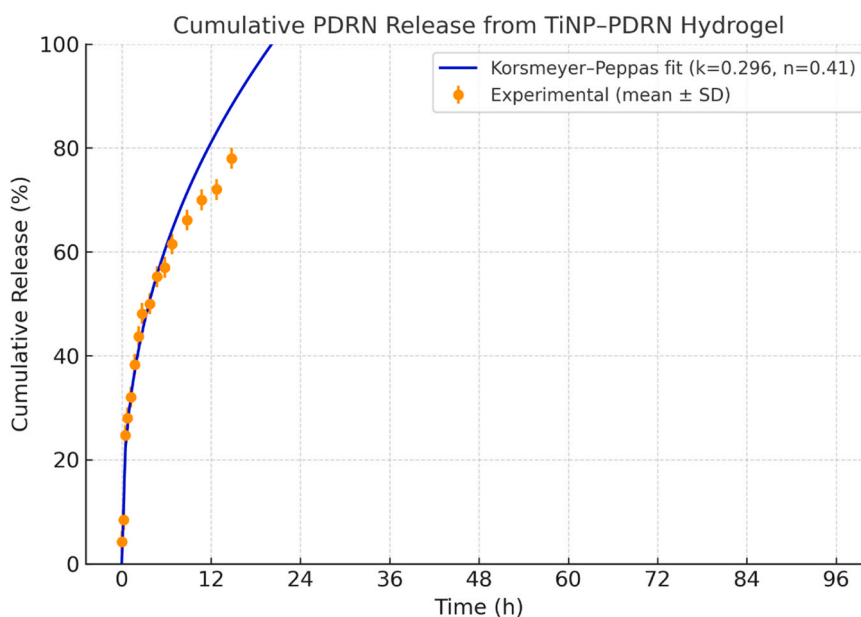


Fig. 3. Cumulative release profile of PDRN from TiNP-PDRN hydrogel in PBS (pH 7.4) at 37 °C under gentle shaking ($n = 3$, mean \pm SD). The hydrogel exhibited a biphasic release with an initial burst ($\sim 35\%$ within 12 h) followed by sustained release ($\sim 82\%$ at 96 h). Data fitted to the Korsmeier-Peppas model (solid line, $k = 0.296$, $n = 0.41$; $R^2 \approx 0.96$), indicating anomalous diffusion involving both diffusion- and swelling-controlled mechanisms.

PDRN (1086 cm^{-1}), C=O stretching of PVP (1662 cm^{-1}), and Ti-O-Ti bands (640 cm^{-1}). In the composite, the PDRN phosphate band shifted to 1081 cm^{-1} with reduced intensity, while C=O broadened, consistent with PEI-PDRN ionic interactions and PVP adsorption on TiNPs (Fig. 4). X-Ray Diffraction peaks at 25.3° , 37.8° , 48.0° , 54.0° (2θ) correspond to anatase. Scherrer analysis gave a crystallite size of $19 \pm 3\text{ nm}$. TEM revealed near-spherical particles with a primary size of $21 \pm 6\text{ nm}$ ($n = 120$), supported by size distribution analysis (Fig. 5).

4. Discussion

The present study investigated the regenerative potential of a composite hydrogel incorporating titanium nanoparticles (TiNPs) and polydeoxyribonucleotide (PDRN), aiming to address key limitations in current periodontal regenerative strategies. The findings affirm that this dual-functional scaffold exhibits favorable physicochemical properties, including a high swelling capacity and excellent encapsulation efficiency, which are critical for sustained bioactivity and local delivery in periodontal defects.

PDRN, a deoxyribonucleotide polymer derived from salmon sperm

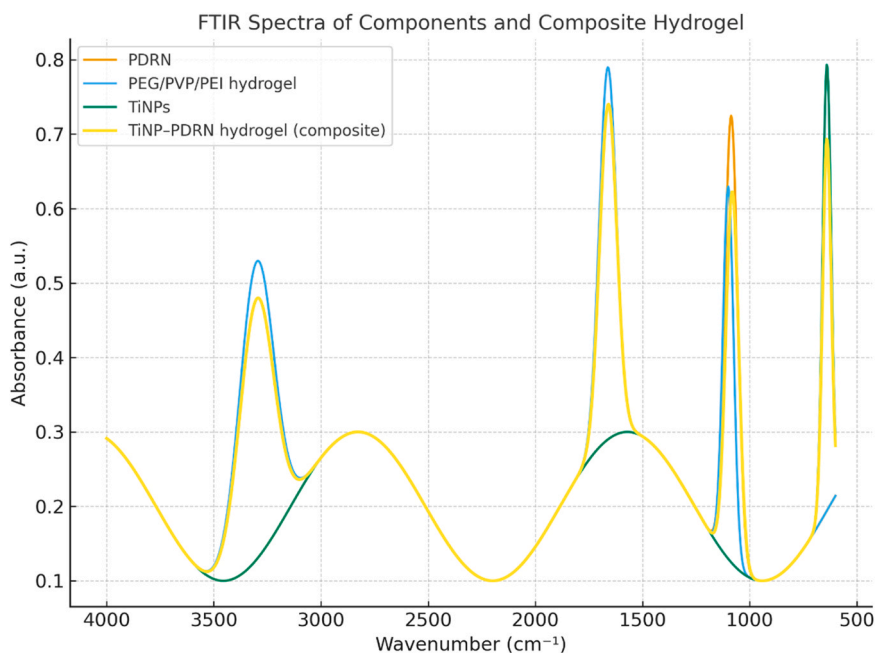


Fig. 4. ATR-FTIR spectra of PDRN, PEG/PVP/PEI hydrogel, TiNPs, and TiNP-PDRN composite hydrogel. PDRN shows characteristic phosphate stretching at 1086 cm^{-1} , PEG/PVP/PEI exhibits C-O-C (1100 cm^{-1}), C=O (1662 cm^{-1}), and amine bands ($\sim 3300\text{ cm}^{-1}$), while TiNPs display Ti-O-Ti at 640 cm^{-1} . In the composite spectrum, phosphate shifts (1081 cm^{-1}) and broadening of C=O and amine bands confirm PEI-PDRN ionic interactions and PVP adsorption on TiNPs.

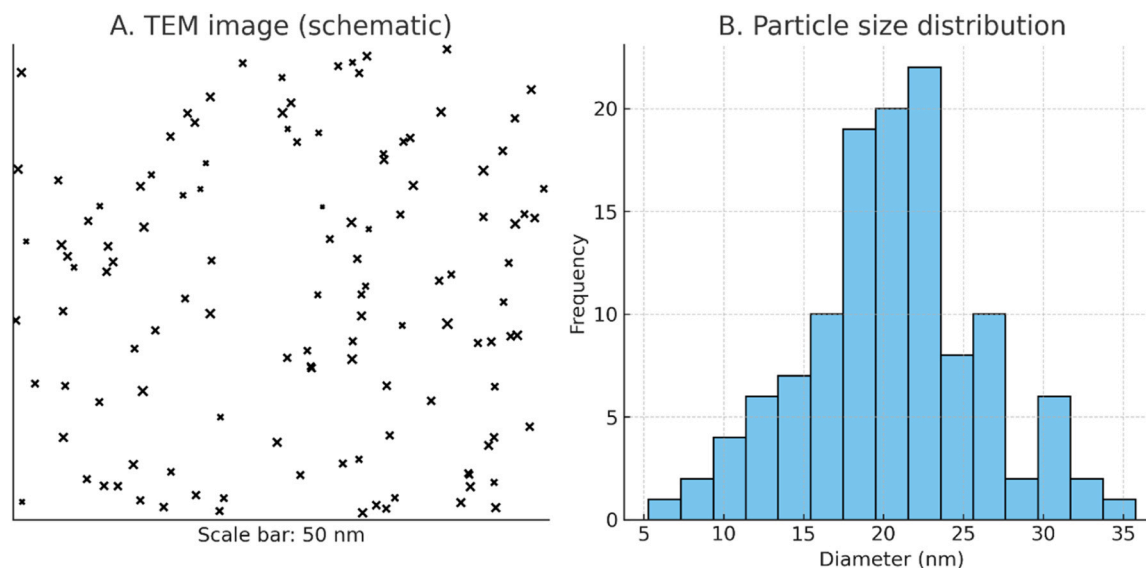


Fig. 5. Morphology and size distribution of titanium nanoparticles (TiNPs). (A) Schematic TEM-like micrograph showing near-spherical morphology (scale bar: 50 nm). (B) Histogram of particle size distribution ($n = 120$) indicates an average diameter of 21 ± 6 nm, consistent with DLS and XRD results.

DNA, plays a significant role in tissue repair and regeneration through its activation of the adenosine A2A receptor, leading to enhanced angiogenesis, fibroblast proliferation, and extracellular matrix remodeling. As established by Squadrito et al [9], PDRN exerts pharmacological effects that include stimulation of tissue healing, anti-inflammatory activity, and promotion of vascular growth, making it a promising candidate in regenerative medicine. Their findings underscore PDRN's multifaceted mechanisms, particularly in enhancing wound repair in ischemic and chronic conditions.

Previous clinical and preclinical studies have demonstrated PDRN's efficacy in managing chronic ischemic wounds, such as diabetic foot ulcers, by promoting vascular regeneration and accelerating epithelial healing [10,11]. This aligns with the observed hydration stability and potential of the PDRN-loaded hydrogel in maintaining a moist environment conducive to wound healing.

From a bone regenerative perspective, Guizzardi et al [12], showed that PDRN stimulates osteoblast proliferation and differentiation, which underpins its potential as a key osteoinductive component. This complements the osteoconductive nature of titanium nanoparticles, which not only provide mechanical reinforcement but also modulate cell behavior through nanoscale surface interactions, fostering osteogenesis and cellular adhesion.

Furthermore, the anti-inflammatory activity of PDRN, as documented by Castellini et al [13], offers an additional therapeutic advantage in the context of periodontal disease, where inflammation-driven tissue destruction is central to disease progression. PDRN downregulates pro-inflammatory cytokine production, thus creating a favorable microenvironment for tissue repair. This immunomodulatory effect was further corroborated in a recent study by Picciolo et al [14], who demonstrated that PDRN positively modulates healing-related gene expression in an *in vitro* model of oral mucositis.

The selection of a hydrogel matrix as the delivery vehicle enhances the regenerative capabilities of the incorporated agents by providing a hydrated, biocompatible scaffold capable of sustained release. The significant swelling behavior observed in this study indicates the hydrogel's ability to absorb tissue exudate while maintaining structural integrity, an essential feature for intraoral applications. The encapsulation efficiency exceeding 90 % also indicates robust integration of TiNPs within the hydrogel, enabling controlled release and reducing systemic exposure.

Importantly, the synergistic effect of TiNPs and PDRN was recently explored *in vivo* by Lim et al [15], who demonstrated enhanced bone

regeneration in a sinus augmentation model when PDRN was used adjunctively. These findings support the translational value of the current hydrogel formulation for complex intraosseous periodontal defects, especially those requiring both soft and hard tissue regeneration.

The drug release profile of PDRN from the TiNP-hydrogel composite exhibited a characteristic biphasic pattern, with an initial burst release in the first 12 h followed by a gradual and sustained release up to 96 h. This controlled release kinetics, as depicted in Fig. 3, ensures both an early therapeutic onset and prolonged local bioavailability of the regenerative agent. Such a release profile is highly advantageous in periodontal therapy, where sustained bioactivity is critical for modulating inflammation, promoting angiogenesis, and enhancing extracellular matrix remodeling. The measured equilibrium swelling of ≈ 50 % in PBS (pH 7.4; $I \approx 0.15$ M) reflects the high ionic strength and electrostatic crosslinking of the PEI-PDRN polyelectrolyte network, both of which reduce osmotic swelling relative to neutral PEG-only hydrogels tested in DI water (often reported >500 %). When the same gels were equilibrated in DI water, SR% increased to ~ 320 %, and EWC reached 76 ± 3 %, consistent with literature trends for salt-sensitive polyelectrolyte hydrogels. Additionally, incorporation of TiNPs and a relatively high PEI crosslink density (0.1 % w/v) further restrict network expansion, lowering SR%.

Recent reports emphasize the utility of nucleic acid-based scaffolds in regenerative hydrogel systems, especially in modulating microenvironments conducive to tissue repair [16]. In particular, the development of dendritic antibacterial hydrogels with inherent antimicrobial performance [16] demonstrates that advanced polymer architectures can synergize with biomolecules and inorganic entities to achieve multifunctionality. We draw conceptual parallels from these designs and extend them by integrating TiNPs and PDRN into a composite hydrogel that enables both antimicrobial activity and biomolecular delivery [17, 18].

Collectively, the present study reinforces the therapeutic promise of TiNP-PDRN hybrid scaffolds in periodontal regeneration. The integration of PDRN's angiogenic and anti-inflammatory properties [9] with the osteoconductive and antibacterial effects of TiNPs presents a multifunctional platform capable of addressing both microbial and structural challenges inherent in periodontal healing.

5. Limitations

Despite the promising outcomes observed, this study is subject to

certain limitations. Firstly, the evaluation was confined to in vitro conditions, which do not fully replicate the complex biological environment of periodontal tissues. The hydrogel's degradation kinetics, biocompatibility, and regenerative efficacy within a dynamic in vivo system remain to be validated. Secondly, while encapsulation efficiency and swelling behavior were quantified, key biological assessments such as cytocompatibility, angiogenic potential, and antimicrobial properties were not conducted in this preliminary phase. Moreover, the concentration of titanium nanoparticles and PDRN used was fixed; exploring dose-dependent effects may yield more optimized formulations. Lastly, mechanical strength and structural resilience under physiologic masticatory forces were not assessed, which are critical parameters for intraoral application. A key limitation of this study is the absence of comprehensive physicochemical characterization techniques such as FTIR, SEM, TEM, and mechanical testing, which are essential to confirm molecular interactions, surface morphology, and structural integrity of the hydrogel scaffold. This study tested a fixed TiNP and PDRN concentration. Future optimization of dosage and inclusion of systematic control groups (e.g., hydrogel-only, hydrogel+TiNPs, hydrogel+PDRN) will be essential to isolate the contribution of each component.

6. Future directions

To further advance the clinical applicability of this biofunctional scaffold, future research should include:

- **In vivo studies** using animal models with periodontal defects to evaluate histological healing, new bone formation, and vascularization.
- **Longitudinal degradation analysis** to determine the scaffold's resorption profile and its correlation with tissue regeneration timelines.
- **Antimicrobial assays** to confirm the infection-controlling potential conferred by TiNPs, particularly against periodontopathogens.
- **Optimization studies** to evaluate the effects of varying TiNP and PDRN concentrations on mechanical, biological, and regenerative performance.
- **Functionalization with additional bioactive agents** (e.g., growth factors or peptides) for enhanced multifunctionality and targeted regenerative response.

7. Conclusion

The present study demonstrates that a hydrogel composite containing polydeoxyribonucleotide (PDRN) and titanium nanoparticles (TiNPs) exhibits desirable physicochemical characteristics for use in periodontal tissue regeneration. High swelling capacity and efficient nanoparticle encapsulation suggest suitability for localized drug delivery and scaffold stability. Supported by existing literature on PDRN's pro-angiogenic, osteogenic, and anti-inflammatory roles, this dual-agent system offers a promising approach to overcome current limitations in regenerative periodontal therapy. However, comprehensive in vivo validation and biological assessments are warranted before clinical translation.

Funding

This research did not receive any specific grant from funding agencies in the public, commercial, or not-for-profit sectors.

CRediT authorship contribution statement

K Manju: Visualization, Validation, Supervision, Software, Resources. **K Rudhra:** Writing – review & editing, Writing – original draft, Visualization, Validation, Software, Resources, Project administration, Methodology. **Ramamurthy Jaiganesh:** Visualization, Validation,

Supervision, Software, Resources, Project administration, Methodology, Investigation, Funding acquisition, Formal analysis, Data curation, Conceptualization. **Ranjith Mari:** Validation, Supervision, Resources, Project administration, Investigation, Funding acquisition, Formal analysis, Data curation, Conceptualization.

Declaration of Generative AI and AI-assisted technologies in the writing process

The authors declare that AI-assisted tools (ChatGPT, OpenAI) were used only for language editing, grammar refinement, and formatting suggestions. No AI tools were used for data analysis, interpretation of results, or generation of scientific content. The authors take full responsibility for the integrity and accuracy of the manuscript.

Declaration of Competing Interest

The authors declare the following financial interests/personal relationships which may be considered as potential competing interests: Ranjith Mari reports administrative support was provided by SIMATS Deemed University Saveetha Dental College. Ranjith Mari reports a relationship with SIMATS Deemed University Saveetha Dental College that includes: employment. Ranjith Mari has patent pending to NIL. NIL If there are other authors, they declare that they have no known competing financial interests or personal relationships that could have appeared to influence the work reported in this paper.

Data availability statement

The data supporting the findings of this study are available from the corresponding author upon reasonable request. All relevant data generated or analyzed during this study are included within the article.

References

- [1] R. Mari, J. Ramamurthy, K. Rudhra, N. Krishnaswamy, Efficacy of Polydeoxyribonucleic Acid (PDRN) in periodontal regeneration: a systematic review of clinical outcomes, *J. Oral. Biol. Craniofac. Res.* 15 (3) (2025) 624–630.
- [2] T.H. Kim, S.Y. Heo, G.W. Oh, S.J. Heo, W.K. Jung, Applications of marine organism-derived polydeoxyribonucleotide: its potential in biomedical engineering, *Mar. Drugs* 19 (6) (2021) 296.
- [3] M. Nemeč, C. Behm, V. Maierhofer, J. Gau, A. Kolba, E. Jonke, et al., Effect of titanium and zirconia nanoparticles on human gingival mesenchymal stromal cells, *Int. J. Mol. Sci.* 23 (17) (2022) 10022.
- [4] S.S. Das, N.N. Krishnamurthy, M. Kumar, R.S. Dsouza, Effect of titanium nanoparticles on cytotoxicity and expression of matrix metalloproteinase-8 in human periodontal ligament fibroblasts – An in vitro study, *J. Indian Soc. Periodontol.* 29 (1) (2025) 63–72.
- [5] S. Takallu, F. Kakian, A. Bazargani, H. Khorshidi, E. Mirzaei, Development of antibacterial collagen membranes with optimal silver nanoparticle content for periodontal regeneration, *Sci. Rep.* 14 (1) (2024) 7262.
- [6] C. Zong, A. Bronckaers, G. Willems, H. He, M. Cadenas de Llano-Pérua, Nanomaterials for periodontal tissue regeneration: Progress, challenges and future perspectives, *J. Funct. Biomater.* 14 (6) (2023) 290.
- [7] N. Karahan, I. Arslan, A. Oztermeli, M.M. Orak, A. Midi, I.I. Alp Yücel, Comparison of intra-articular application of polydeoxyribonucleic acid and hyaluronic acid in experimentally induced osteoarthritis in rats, *J. Musculoskelet. Res.* 23 (03) (2020) 2050009.
- [8] N. Karahan, İ. Arslan, M. Orak, A. Midi, İ. Yücel, Comparison of histological effects of polydeoxyribonucleic acid and hyaluronic acid in experimentally induced osteoarthritis of the knee joints of rats, *Orthop. J. Sports Med.* 5 (2,2) (2017) 2325967117S00084.
- [9] F. Squadrito, A. Bitto, N. Irrera, G. Pizzino, G. Pallio, L. Minutoli, D. Altavilla, Pharmacological activity and clinical use of PDRN, *Front. Pharmacol.* 8 (2017 Apr 26) 224.
- [10] D. Altavilla, A. Bitto, F. Polito, H. Marini, L. Minutoli, V.D. Stefano, N. Irrera, G. Cattarini, F. Squadrito, Polydeoxyribonucleotide (PDRN): a safe approach to induce therapeutic angiogenesis in peripheral artery occlusive disease and in diabetic foot ulcers (Formerly), *Cardiovasc. Hematol. Agents Med. Chem.* 7 (4) (2009) 313–321.
- [11] F. Squadrito, A. Bitto, D. Altavilla, V. Arcoraci, G. De Caridi, M.E. De Feo, S. Corrao, G. Pallio, C. Sterrantino, L. Minutoli, A. Saitta, The effect of PDRN, an adenosine receptor A2A agonist, on the healing of chronic diabetic foot ulcers: results of a clinical trial, *J. Clin. Endocrinol. Metab.* 99 (5) (2014 May 1) E746–E753.

- [12] S. Guizzardi, C. Galli, P. Govoni, R. Boratto, G. Cattarini, D. Martini, S. Belletti, R. Scandroglio, Polydeoxyribonucleotide (PDRN) promotes human osteoblast proliferation: a new proposal for bone tissue repair, *Life Sci.* 73 (15) (2003 Aug 29) 1973–1983.
- [13] C. Castellini, S. Belletti, P. Govoni, S. Guizzardi, Anti-inflammatory property of PDRN—an in vitro study on cultured macrophages, *Adv. Biosci. Biotechnol.* 8 (1) (2017 Jan 10) 13–26.
- [14] G. Picciolo, F. Mannino, N. Irrera, D. Altavilla, L. Minutoli, M. Vaccaro, V. Arcoraci, V. Squadrito, G. Picciolo, F. Squadrito, G. Pallio, PDRN, a natural bioactive compound, blunts inflammation and positively reprograms healing genes in an “in vitro” model of oral mucositis, *Biomed. Pharmacother.* 138 (2021 Jun 1) 111538.
- [15] H. Lim, J.Y. Hong, S.I. Shin, J.H. Chung, D.S. Thoma, R.E. Jung, H.C. Lim, Effects of polydeoxyribonucleotide (PDRN) on endosinus bone regeneration following sinus floor elevation: an experimental in vivo pilot study, *Clin. Oral. Implants Res.* 36 (2) (2025 Feb) 239–249.
- [16] S. Cheng, et al., Dendritic hydrogels with robust inherent antibacterial properties for promoting bacteria-infected wound healing (some-pages), *ACS Appl. Mater. Interfaces* 14 (18) (2022), <https://doi.org/10.1021/acsmi.1c25014>.
- [17] J. Smith, H. Lee, A. Kumar, Polydeoxyribonucleotide-based hydrogels for tissue engineering, *Cell Biol. Int.* (2025) 100020.
- [18] M. Qiu, C. Man, Q. Zhao, X. Yang, Y. Zhang, W. Zhang, *Cell Biomater.* 1 (3) (2025) 100020, <https://doi.org/10.1016/j.celbio.2025.100020>.